

# Evaluation of Long-Lasting Potential of Suprachoroidal Axitinib Suspension Via Ocular and Systemic Disposition in Rabbits

Viral S. Kansara<sup>1</sup>, Leroy W. Muya<sup>1</sup>, and Thomas A. Ciulla<sup>1</sup>

<sup>1</sup> Clearside Biomedical Inc., Alpharetta, GA, USA

**Correspondence:** Thomas A. Ciulla, Clearside Biomedical Inc., 900 Northpoint Parkway Suite 200, Alpharetta, GA 30005, USA. e-mail: [thomas.ciulla@clearsidebio.com](mailto:thomas.ciulla@clearsidebio.com)

**Received:** November 23, 2020

**Accepted:** March 15, 2021

**Published:** June 15, 2021

**Keywords:** suprachoroidal injection; receptor tyrosine kinase inhibitor; axitinib; VEGF; pharmacokinetics; AMD; intravitreal

**Citation:** Kansara VS, Muya LW, Ciulla TA. Evaluation of long-lasting potential of suprachoroidal axitinib suspension via ocular and systemic disposition in rabbits. *Transl Vis Sci Technol.* 2021;10(7):19. <https://doi.org/10.1167/tvst.10.7.19>

**Purpose:** Axitinib, a tyrosine kinase inhibitor, is a potent inhibitor of vascular endothelial growth factor (VEGF) receptors –1, –2 and –3. Suprachoroidal (SC) delivery of axitinib, combined with pan-VEGF inhibition activity of axitinib, has the potential to provide additional benefits compared to the current standard of care with intravitreal anti-VEGF-A agents. This study evaluated the ocular pharmacokinetics and systemic disposition of axitinib after SC administration in rabbits.

**Methods:** Rabbits received axitinib as either a single SC injection (0.03, 0.10, 1.00, or 4.00 mg/eye;  $n = 4$ /group) or a single intravitreal injection (1 mg/eye;  $n = 4$ /group) in three separate studies. Axitinib concentrations were measured in several ocular compartments and in plasma at predetermined timepoints for up to 91 days. The pharmacokinetics parameters were estimated by noncompartmental analysis.

**Results:** A single SC injection of axitinib suspension (1 mg/eye) resulted in an 11-fold higher mean axitinib exposure in the posterior eye cup, compared with intravitreal injection. Sustained levels of axitinib in the retinal pigment epithelium–choroid–sclera (RCS) and retina were observed throughout the duration of studies after a single SC axitinib injection (0.1 and 4.0 mg/eye), with low exposure in the vitreous humor, aqueous humor, and plasma. Axitinib levels in the RCS were 3 to 5 log orders higher than the reported in vitro (VEGF receptor–2 autophosphorylation inhibition) 50% inhibitory concentration value after 0.1 and 4.0 mg/eye dose levels throughout the 65-day and 91-day studies, respectively.

**Conclusions:** This study demonstrates that SC axitinib suspension has a favorable pharmacokinetics profile with potential as a long-acting therapeutic candidate targeted to affected choroid and retinal pigment epithelium in neovascular age-related macular degeneration.

**Translational Relevance:** Suprachoroidal axitinib suspension has potential to decrease the treatment burden in neovascular age-related macular degeneration, as a long-acting therapeutic candidate, and could yield greater efficacy, as a potent tyrosine kinase pan-VEGF inhibitor, compared with current standard anti-VEGF-A therapies.

## Introduction

Neovascular age-related macular degeneration (nAMD) is the leading cause of vision loss in the industrialized world.<sup>1–3</sup> It is caused by abnormal blood vessel growth generally originating in the choriocapillaris, a layer of capillaries situated immediately below the retinal pigment epithelium (RPE)/Bruch's

membrane. This aberrant choroidal neovascularization is driven by the upregulation of cytokines involved in angiogenesis, particularly vascular endothelial growth factor-A (VEGF-A).<sup>4,5</sup> Currently, intravitreal (IVT) anti-VEGF-A drugs are the standard of care for the treatment of nAMD<sup>6</sup>; however, the therapeutic benefit of these drugs is suboptimal, and the need remains for new drugs and delivery methods to improve and maintain visual acuity.<sup>7–9</sup> In addition, long-term

real-world outcomes of anti-VEGF therapy, at 4, 5, and 7 years<sup>10,11</sup> are worse, which may, in part, be due to the treatment burden of multiple visits on patients, caregivers, and physicians. For those patients with an incomplete response to anti-VEGF-A therapy, there is both an interest and a need for new drugs and delivery methods to improve and maintain visual acuity.

Axitinib, a second-generation receptor tyrosine kinase inhibitor, inhibits VEGF receptors VEGFR-1, VEGFR-2, and VEGFR-3 at picomolar concentrations<sup>12</sup> by stabilizing the receptor kinase domain in an inactive conformation. Multiple *in vivo* studies in mouse, rat, and rabbit models support the potential activity of axitinib for the treatment of neovascularization in corneal, retinal, and choroidal tissues.<sup>13–18</sup> The biological activity of suprachoroidally delivered axitinib has been demonstrated in a laser-induced choroidal neovascularization model, and retinal vascular leakage model, in rats and pigs.<sup>19,20</sup>

Owing to its potent pan-VEGFR inhibition, axitinib may provide a meaningful benefit compared with current anti-VEGF-A agents, which leads to the upregulation of VEGF-C and VEGF-D.<sup>21,22</sup> This upregulation of other VEGF ligands could contribute to tachyphylaxis, a form of treatment resistance, and may lead to refractory cases clinically. This potential benefit of pan-VEGF inhibition over focused VEGF-A inhibition is supported by studies in which axitinib more effectively inhibited angiogenic sprouts than a VEGF-A inhibitor.<sup>14</sup> Similarly, a recent phase II clinical trial demonstrated that broad VEGF inhibition yielded a statistically significantly better visual outcome in nAMD than focused VEGF-A inhibition.<sup>23</sup>

Microneedle-based suprachoroidal (SC) injection is a minimally invasive office-based procedure performed in the pars plana that delivers therapeutics into the SC space (SCS).<sup>24–28</sup> Compared with IVT injection, SC delivery of axitinib suspension may provide targeted and compartmentalized drug delivery to the affected choroid and RPE, and spare most of the globe (vitreous, lens, aqueous humor, and cornea), potentially minimizing off-target effects. This targeted method of delivery may result in high and sustained delivery of axitinib to the choroid and RPE in nAMD, to potentially maximize efficacy, while simultaneously maintaining low systemic exposure to potentially enhance safety. This delivery technique has been validated in a phase III clinical trial of a corticosteroid for the treatment of uveitic macular edema.<sup>29</sup> A recent study assessed physician–investigator experience with microneedle-based SC injection across six clinical trials and three disease states.<sup>30</sup> A user survey

was conducted, along with a retrospective correlation analysis between procedural variables, demographics, and ocular characteristics. This study demonstrated that microneedle-based SC injection is well accepted by physician–investigators, and that it can accommodate a wide range of anatomic and demographic variables.

Axitinib, with its pan-VEGF inhibition activity,<sup>14</sup> may have therapeutic synergies with SC delivery, with its ability to target affected posterior tissues and compartmentalize drug away from unaffected tissues.<sup>24–28</sup> Specifically, SC administered axitinib suspension has the potential to address challenges currently experienced by patients with nAMD and health care providers, such as treatment burden, suboptimal dosing and limited outcomes or drug resistance.<sup>10,11</sup> Therefore, the objective of this research was to assess the ocular pharmacokinetics (PK), and systemic disposition of axitinib after SC administration in rabbits. Ocular levels of axitinib after microneedle-based SC administration were compared with those following clinically accepted IVT administration.

## Methods

### Injectable Suspension Formulation of Axitinib

Axitinib, a poorly aqueous-soluble small molecule (0.2 µg/mL at physiological pH) with a molecular weight of 386.5 g/mol, was micronized ( $D_{50}$ : <3 µm and  $D_{90}$ : <5 µm) and compounded as a stable injectable opaque-white ophthalmic suspension ( $D_{10}$ : <3 µm,  $D_{50}$ : <7 µm and  $D_{90}$ : <10 µm) at physiological pH using polysorbate 80, a wetting agent, before the addition of a phosphate-buffered suspending solution containing sodium carboxymethylcellulose, a viscosity-enhancing agent, and sodium chloride, a tonicity agent, and pH adjusted to neutral pH using either 1N sodium hydroxide or 1N hydrochloric acid. The suspension formulations were prepared at 10 and 40 mg/mL concentrations, and further diluted with the placebo formulation vehicle to achieve the desired lower concentrations (0.3, 1.0, and 4.0 mg/mL). The suspension was then terminally sterilized and the final concentration of axitinib was confirmed via a high-performance liquid chromatography assay. All formulations were stored at room temperature and protected from light. Immediately before dosing, each test article was vortexed for approximately 2 minutes.

**Table 1.** Outline of the In Vivo Study Design

Study Number	Study Size, Species	Delivery Route	Injection Volume (Concentration)	Dose* (mg/Eye)	Study Duration (Weeks)	PK Timepoints After the Dose
1	<i>n</i> = 10 male NZW rabbits	IVT SC	0.025 mL (4 mg/mL) 0.1 mL (10 mg/mL)	1 1	1	0.08, 6, 24, 72, and 168 hours
2	<i>n</i> = 14 male DB rabbits	SC	0.1 mL (40 mg/mL)	4	13	2, 4, 8, 15, 29, 61, and 91 days
3	<i>n</i> = 14 male DB rabbits	SC	0.1 mL (1 mg/mL) 0.1 mL (0.3 mg/mL)	0.1 0.03	10	2, 8, 15, 31, 45, 61, and 66 (±1) days

NZW, New Zealand White; DB, Dutch Belted.

\*Both eyes of each animal were dosed. All animals were free of ophthalmologic abnormalities before test article administration, assessed by a board-certified veterinary ophthalmologist using a slit lamp biomicroscope and an indirect ophthalmoscope.

## In Vivo Studies

### Institutional Animal Care and Use Committee Compliance

Animal care and use during the study was conducted in accordance with the regulations of the USDA Animal Welfare Act (the Code of Federal Regulations 3), and according to the CRO's in-house Institutional Animal Care and Use Committee. All animals were treated in accordance with the ARVO Statement for the Use of Animals in Ophthalmic and Vision Research.

### Study Design and Rationale

Table 1 presents an outline of the three different studies conducted to evaluate the ocular PK, disposition, and tolerability of axitinib injectable suspension in rabbits. Rabbits were selected for the relatively large size of their eyes, which are amenable to reliable SC injection. Moreover, rabbits have been a species of choice to study ocular PK of various therapeutic agents.<sup>31–33</sup> In the first study (study 1), the ocular PK of the axitinib suspension depot (1 mg/eye) after SC injections was compared with that after IVT injection. In the second study (study 2), the durability of axitinib levels in posterior segment tissues was assessed after a single bilateral SC administration of axitinib suspension depot (4 mg/eye). Axitinib is a potent inhibitor of VEGFR2 with picomolar inhibitory concentration and therefore, in study 3, ocular PK and systemic disposition of axitinib at potentially clinically relevant doses (0.03 and 0.10 mg/eye) were assessed.

### Animal Screening, Randomization, Care, and Treatment

New Zealand White (*Oryctolagus cuniculus*) male rabbits (2.3–2.9 kg) were obtained from the West Oregon Rabbit Company and acclimated in designated housing for 5 days before dosing. Male Dutch Belted [Haz:(DB)SPF] rabbits (5 months, 1.7–1.9 kgs) were acclimated to study conditions for up to 16 days before dose administration. All animals were screened based on health conditions, general observations, body weight, and predose ophthalmic examinations performed by a single assessor per study in a masked manner. Study 1 animals were assigned based on weight using a Latin square design. Study 2 and study 3 animals were assigned to various groups in sequential order based on the original number assigned upon their arrival.

### Dosing Procedures

Rabbits were anesthetized immediately before dosing per approved Institutional Animal Care and Use Committee and standard operating procedures. Before dosing, 1 drop of topical proparacaine hydrochloride anesthetic (0.5%) was administered to each eye, and the eyes were rinsed with an iodine solution followed by a saline rinse. All the injections were performed by a board-certified experienced veterinary ophthalmologist.

**Intravitreal Injection.** A single intravitreal injection (0.025 mL) was performed approximately 4 mm posterior to the limbus using a 30G hypodermic needle. The needle placement was at the 11 or 1 o'clock

position. The needle was inserted at a 45° angle toward the back of the eye to avoid damaging the lens. The formulation was then injected slowly after confirming the tips of the needle in the mid-vitreous humor via direct visual examination. After the injection, the needle was kept in the eye for approximately 20 seconds before being withdrawn to avoid any potential reflux. Upon withdrawal of the microneedle, a cotton-tipped applicator was placed over the injection site for approximately 10 seconds. The axitinib formulation (40 mg/mL) was administered into both eyes (1 mg/eye) of each animal. The formulation delivery into the midvitreous was confirmed via indirect ophthalmoscopy.

**SC Injection.** A single SC injection (0.1 mL) was administered 4.0 to 4.5 mm from the limbus in the superior temporal quadrant via a tuberculin syringe with a proprietary 30G microneedle 700 μm in length (Clearside Biomedical, Alpharetta, GA). The needle was inserted into the sclera at a perpendicular angle to the injection location, gentle force was then applied to the syringe so that the hub of the needle contacts and subsequently depresses the globe of the eye, creating a sealing gasket effect between the hub of the needle and the conjunctiva. This sealing gasket effect ensures that the needle opening reaches the SCS, while minimizing reflux during the injection. When the needle advanced inward past the sclera, a loss of resistance was felt with the advancement of the plunger of the device, initiating delivery of the axitinib suspension into the SCS over approximately 5 to 10 seconds to each eye. After the completion of dose administration, the needle was kept in the eye for approximately 20 seconds before being withdrawn to avoid any potential reflux. Upon withdrawal of the microneedle, a cotton-tipped applicator was placed over the injection site for approximately 10 seconds. The axitinib formulations at concentrations of either 40 mg/mL, 10 mg/mL, or 3 mg/mL were administered into both eyes of each animal to achieve 4.0 mg/eye, 0.1 mg/eye, and 0.03 mg/eye dose levels, respectively. The right eye was dosed first; all postdose times were based on the time of dosing of the second (left) eye.

### Sample Collection and Bioanalysis

Blood samples were collected from each animal either via an ear vessel before euthanasia or via cardiac puncture. Approximately 1 mL samples were collected and placed into tubes containing sodium heparin as the anticoagulant. Samples were maintained on wet ice until centrifuged to obtain plasma. Plasma

samples were stored frozen at approximately  $-70^{\circ}\text{C}$  until analyzed.

Animals were euthanized at the designated time points by overdose using sodium pentobarbital (150 mg/kg, IV, approximately 5 mL). Both eyes ( $n = 4$  eyes from two rabbits per timepoint) were enucleated immediately after euthanasia. The aqueous humor was collected fresh, and each eye was flash frozen in liquid nitrogen for 15 to 20 seconds, and subsequently placed on dry ice for at least 2 hours, and stored at  $-70^{\circ}\text{C}$ . The eyes were dissected to collect the retina, RPE–choroid–sclera complex (RCS) or posterior eye cup (PEC). The vitreous humor was collected via frozen dissection. The ocular tissues were rinsed with saline and blotted dry, as appropriate, weighed, and placed on dry ice until stored at approximately  $-70^{\circ}\text{C}$  until analyzed. Samples were analyzed for concentrations of axitinib using the liquid chromatography/tandem mass spectrometry.

### Data Analysis and PK Analysis

Unless otherwise noted, calculated values for mean and standard deviation are reported to three significant figures. Statistical analyses were limited to descriptive statistics such as mean and standard deviation. The PK parameters were calculated by a noncompartmental method, based on mean concentrations, using Phoenix WinNonlin, version 6.2.1 (Pharsight Corporation, Mountain View, CA). The PK parameters included area under the concentration–time curve from time 0 to the last measurable time point ( $\text{AUC}_{0-t}$ ), the maximum concentration ( $C_{\text{max}}$ ) in plasma, aqueous humor, retina, RCS, and vitreous humor, and the time to reach maximum concentration ( $T_{\text{max}}$ ). Areas under the curve (AUC) were estimated by a linear–trapezoidal method.

## Results

### Comparison of Ocular PK Profiles After SC or IVT Injection

The ocular distribution and systemic disposition of axitinib were assessed and compared after bilateral injection of axitinib (1 mg/eye) after either intravitreal or SC administration in New Zealand White rabbits as described in Table 1, study 1. The mean concentration versus time profiles for ocular tissues are presented graphically in Figure 1. The PK parameters for axitinib in ocular tissues are presented in Table 2.

Axitinib was detected in PEC and vitreous humor at all timepoints after IVT and SC injection of

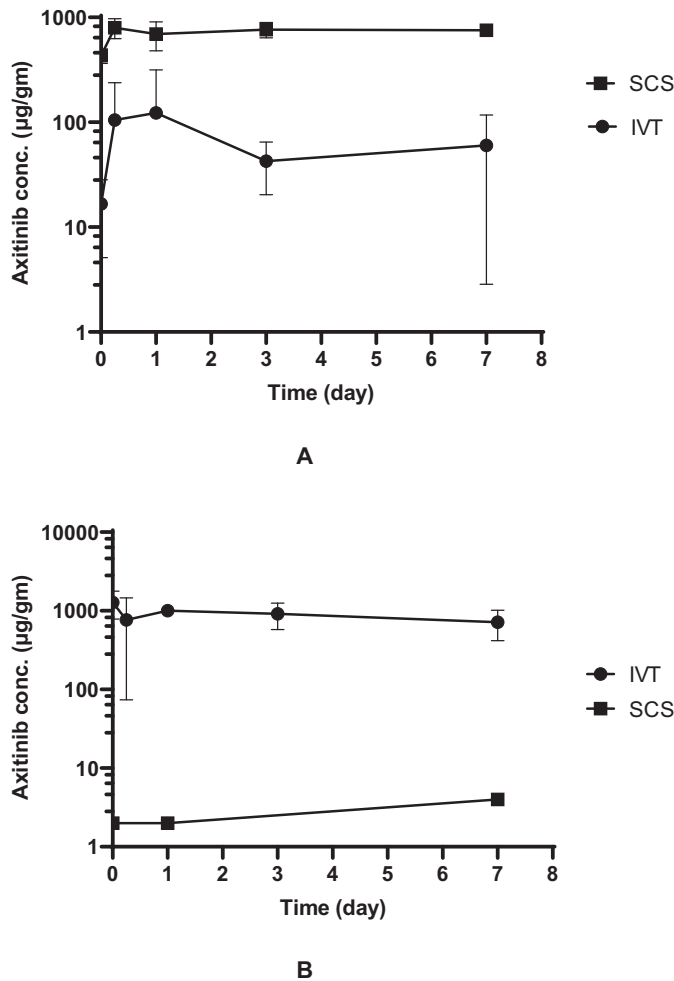


**Figure 1.** Concentration–time profiles of axitinib in the PEC (A) and vitreous humor (B) after a single bilateral administration of axitinib suspension (1 mg/eye) via SC injection and IVT injection in New Zealand White rabbits ( $n = 4$  eyes/2 rabbits/time point). Axitinib was detected in one sample of vitreous humor each on days 0.003, 1, and 7 after SC administration. Missing data points represent axitinib levels below level of detection at respective timepoints. Data are presented as mean  $\pm$  SD. Error bars smaller than the symbol size are not seen on the graph. The axitinib levels in the PEC were statistically different after SC and IVT administration, determined using a two-sided, two-independent  $t$  test at each timepoint, with the  $P$  values of  $<0.001$ ,  $<0.001$ ,  $0.007$ ,  $0.001$ , and  $<0.001$  for the 0.003-, 0.8-, 1-, 3-, and 7-day timepoints, respectively.

**Table 2.** Estimated Pharmacokinetic Parameters of Axitinib in the PEC and Vitreous Humor After a Single Bilateral SC or Intravitreal Injection of Axitinib Suspension (1 mg/Eye) in New Zealand White Rabbits

	PEC		Vitreous Humor	
	SC	IVT	SC	IVT
$AUC_{(0-t)}$ ( $\mu\text{g}\cdot\text{d}/\text{g}$ )	5208	471	19	6208
$C_{\text{max}}$ ( $\mu\text{g}/\text{g}$ )	799	124	3.67	1280
$T_{\text{max}}$ (h)	6	24	168	0.08

axitinib suspension. In the PEC, the mean exposures ( $AUC_{0-t}$ ) were  $5208 \mu\text{g}\cdot\text{d}/\text{g}$  and  $471 \mu\text{g}\cdot\text{d}/\text{g}$ , and the mean  $C_{\text{max}}$  were  $799 \mu\text{g}/\text{g}$  and  $124 \mu\text{g}/\text{g}$  after SC injection and IVT injection, respectively. A reverse trend was observed for axitinib exposure in the vitreous humor. The mean  $AUC_{0-t}$  were  $19 \mu\text{g}\cdot\text{d}/\text{g}$  and  $6208 \mu\text{g}\cdot\text{d}/\text{g}$ , and mean  $C_{\text{max}}$  were  $3.67 \mu\text{g}/\text{g}$  and  $1280 \mu\text{g}/\text{g}$  after SC injection and IVT injection, respectively.

Plasma concentrations of axitinib were below the limit of quantitation (LOQ,  $0.150 \text{ ng}/\text{mL}$ ) for both routes of administration at all timepoints, except at 6 hours after SC administration. These detectable levels of axitinib ( $0.288 \text{ ng}/\text{mL}$  and  $0.155 \text{ ng}/\text{mL}$ ) were close to the LOQ. Overall, negligible levels of axitinib reached systemic circulation after either SC or IVT injection in the eye.

### Durability of Axitinib Ocular Exposure After SC Injection

The durability of axitinib suspension (4 mg axitinib/eye) for up to 3 months after a single bilateral SC injection of axitinib suspension in DB pigmented rabbits (Table 1, study 2) was assessed. The PK parameters for axitinib in ocular tissues are presented in Table 3.

After a single bilateral SC administration of axitinib suspension (4 mg/eye), axitinib was quantifiable at all time points in the RCS, retina, and vitreous humor throughout the study (91 days). Conversely, axitinib was not detected in either plasma (LOQ,  $0.15 \text{ ng}/\text{mL}$ ) or aqueous humor samples (LOQ,  $1 \text{ ng}/\text{mL}$ ). Approximately 61% of the administered dose was recovered on day 91, indicating sustained retention of a drug depot in the SCS for many months (Fig. 2). Axitinib concentrations in RCS were highest ( $C_{\text{max}}$ ,  $22000 \mu\text{g}/\text{g}$ ) early in the study as expected, and slowly declined beyond study day 4 (Fig. 3). The observed mean  $AUC_{0-t}$  of the dose depot was  $1,260,000 \mu\text{g}\cdot\text{d}/\text{g}$  with estimated terminal half-life of 143 days, indicating sustained and high levels of axitinib in the posterior segment tissues.

Axitinib levels in the retina increased over time, to a  $C_{\text{max}}$  of  $325 \mu\text{g}/\text{g}$ , and maintained similar to the  $C_{\text{max}}$  through study ( $305 \mu\text{g}/\text{g}$  on day 91), resulting in the mean  $AUC_{0-t}$  of  $23800 \mu\text{g}\cdot\text{d}/\text{g}$ . The levels of axitinib in the vitreous humor, assuming density of the vitreous humor to be 1, was 3 to 4 log orders lower than that of the RCS and retina. Axitinib was not quantifiable in either plasma (LOQ,  $0.15 \text{ ng}/\text{mL}$ ) or aqueous humor (LOQ,  $1 \text{ ng}/\text{mL}$ ) samples throughout the duration of the study.

**Table 3.** Estimated Pharmacokinetic Parameters of Axitinib in Ocular Tissues After a Single Bilateral SC Injection of Axitinib Suspension (4 mg/Eye) in Dutch-Belted Rabbits

Matrix	AUC <sub>(0-t)</sub> (µg·d/g or µg*d/mL)	C <sub>max</sub> (µg/g or µg/mL)	T <sub>max</sub> (day)
RCS	1,260,000	22,000	4
Retina	23,800	325	61
Vitreous humor	31.1	0.858	4

NC, not calculable.

**Table 4.** Estimated Pharmacokinetic Parameters of Axitinib in Ocular Tissues After a Single Bilateral SC Injection of Axitinib Suspension (0.03 and 0.1 mg/Eye) in Dutch-Belted Rabbits

Dose (mg/eye)	Matrix	AUC <sub>(0-t)</sub> (µg·d/g or µg·d/mL)	C <sub>max</sub> (µg/g or µg/mL)	T <sub>max</sub> (day)
0.03	RCS	338	37.2	1
	Retina	17.3	4.48	1
	Vitreous humor	NC	0.00401	1
0.1	RCS	2320	232	1
	Retina	28.1	6.26	1
	Vitreous humor	NC	0.00458	1

AUC<sub>(0-t)</sub>, area under the curve until the last measurable concentration; C<sub>max</sub>, observed maximum concentration; T<sub>max</sub>, time to C<sub>max</sub>; NC, not calculable.

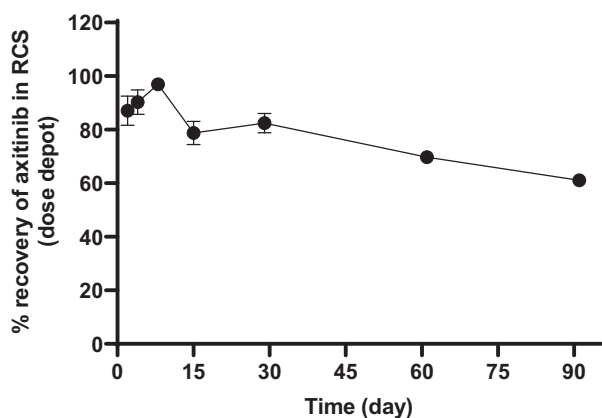


**Figure 2.** Axitinib dose depot recovery (% of dose administered) from RCS after a single administration of axitinib suspension (4 mg/eye) via SC injection in Dutch-Belted rabbits ( $n = 4$  eyes/2 rabbits/time point). Data are presented as mean  $\pm$  SD. Error bars smaller than the symbol size are not seen on the graph.

In a separate 30-week rabbit toxicology study (see supplement), mean axitinib levels measured 199 µg/gm and 1.1 µg/gm in the RCS and retina, respectively, on day 182 after a single 1.05 mg/eye SC injection.

## Ocular PK and Disposition of Axitinib After SC Injection

Ocular PK and systemic disposition of axitinib was assessed at 0.03 mg/eye and 0.1 mg/eye dose levels after

a single bilateral SC injection in DB pigmented rabbits (study 3, Table 1). The PK parameters for axitinib in ocular tissues are presented in Table 4. The mean concentration versus time profiles for ocular tissues are presented in Figure 4.

Axitinib was quantifiable in the RCS samples at both dose levels (0.03 and 0.10 mg/eye) throughout the study. Axitinib levels in RCS reached a C<sub>max</sub> of 37.2 µg/g and 232 µg/g on study day 2 (T<sub>max</sub> = 24 hours after the dose), and generally decreased through study day 66 with estimated terminal half-life of 11 days and 16 days, for the 0.03 mg/eye and 0.1 mg/eye dose levels, respectively. The mean C<sub>max</sub> and AUC<sub>0-∞</sub> values after the 0.10 mg dose were approximately 6-fold and 7-fold higher than that of after 0.03 mg dose, respectively, suggesting that drug depot exposure may not be dose proportional (dose ratio of 3.33).

The mean exposures (AUC<sub>0-t</sub>) of axitinib in the retina were 17.3 and 28.1 µg·d/g for the 0.03 and 0.10 mg/eye doses, respectively. Although axitinib was detected in the RCS at all time points, axitinib concentrations were quantifiable in the retina sporadically on study days 15, 31, 45, 61, and 65. The concentration and exposure ratios for these two dose levels were less than dose proportion. Axitinib levels were quantifiable in the vitreous humor on study day 2, and in only a few eyes in each group on study day 8 and below level of detection on day 15 or later. Axitinib was not quantifiable either in the aqueous humor (LOQ,

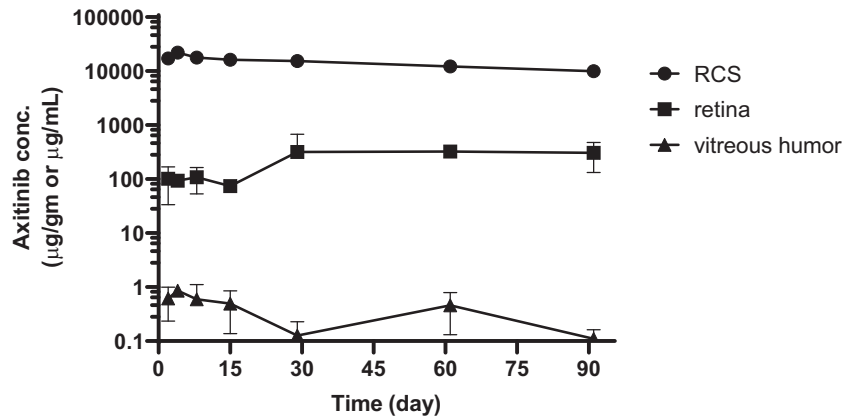


**Figure 3.** Concentration–time profiles of axitinib in the RCS, retina, and vitreous humor after a single bilateral administration of axitinib suspension (4 mg/eye) via SC injection in Dutch-Belted rabbits ( $n = 4$  eyes/2 rabbits/time point). Data are presented as mean  $\pm$  SD. Error bars smaller than the symbol size are not seen on the graph.

1 ng/mL) or plasma (LOQ, 0.15 ng/mL) at any timepoint throughout the study.

## Discussion

Axitinib has several desirable characteristics as a therapeutic candidate, including its high potency against pan-VEGF receptors, with well-established antiangiogenesis and antipermeability mechanisms in *in vitro* studies.<sup>12,34</sup> Axitinib more potently inhibited murine corneal neovascularization than other tyrosine kinase inhibitors, including sorafenib and sunitinib.<sup>16</sup> In a laser photocoagulation-induced choroidal neovascularization model, axitinib treatment in mice<sup>13</sup> and rats<sup>14</sup> caused the regression of established choroidal neovascularization, which may be more clinically relevant than inhibiting choroidal neovascularization. Furthermore, *in vitro* assessment of axitinib revealed better biocompatibility with ocular cells compared with other tyrosine kinase inhibitors,<sup>35</sup> suggesting potential safety benefits.

The limitations of current anti-VEGF-A therapies, such as treatment burden<sup>10,11,36–39</sup> and ceiling effect,<sup>40–43</sup> in the management of nAMD has been highlighted by large real-world retrospective clinical studies. Topical delivery of several tyrosine kinase inhibitors, such as TG100801,<sup>44</sup> pazopanib,<sup>45</sup> regorafenib,<sup>46</sup> and acrizanib,<sup>47</sup> resulted in suboptimal clinical efficacy. More recently, IVT administered sustained release formulations of sunitinib and axitinib have shown preliminary efficacy and safety in phase I/IIa studies for the treatment of patients with nAMD. However, the translocation of particles to the anterior

chamber,<sup>48–50</sup> drug-related off-target effects such as keratopathy,<sup>51–52</sup> and corneal keratic precipitates<sup>53</sup> have been reported in phase I/IIa studies. Although these adverse events could possibly be related to the formulation, there are common trends of migration of particles or corneal off-target effects, underscoring unmet needs.

Microneedle-based SC injection can compartmentalize the drug in the SCS, away from the vitreous and minimize drug exposure to the anterior chamber. It was therefore hypothesized that compartmentalized delivery of axitinib suspension via a microneedle-based technique, in combination with the pan-VEGF inhibition activity of axitinib, would result in high and sustained levels of axitinib in the affected choroid and RPE. Hence, we assessed ocular PK, tissue distribution, and systemic disposition of axitinib after microneedle-based SC delivery of axitinib suspension in rabbits.

In study 1, ocular exposure of axitinib after SC injection of axitinib suspension (1 mg/eye) was compared with that of after the IVT injection. Administration via SC injection resulted in significantly higher exposure (11-fold and 6.4-fold higher  $AUC_{0-t}$  and  $C_{max}$ , respectively) of axitinib in the PEC and lower exposure in the vitreous humor compared with that of after IVT administration. As expected, IVT injection resulted in higher vitreous humor levels of axitinib compared with that after SC injection. These data underscore the potential of compartmentalized delivery of axitinib to affected choroid and RPE (desired site of action), while sparing the vitreous humor, and aqueous humor, which may result in improved efficacy and reduced drug-related toxicity in the anterior segment tissues.

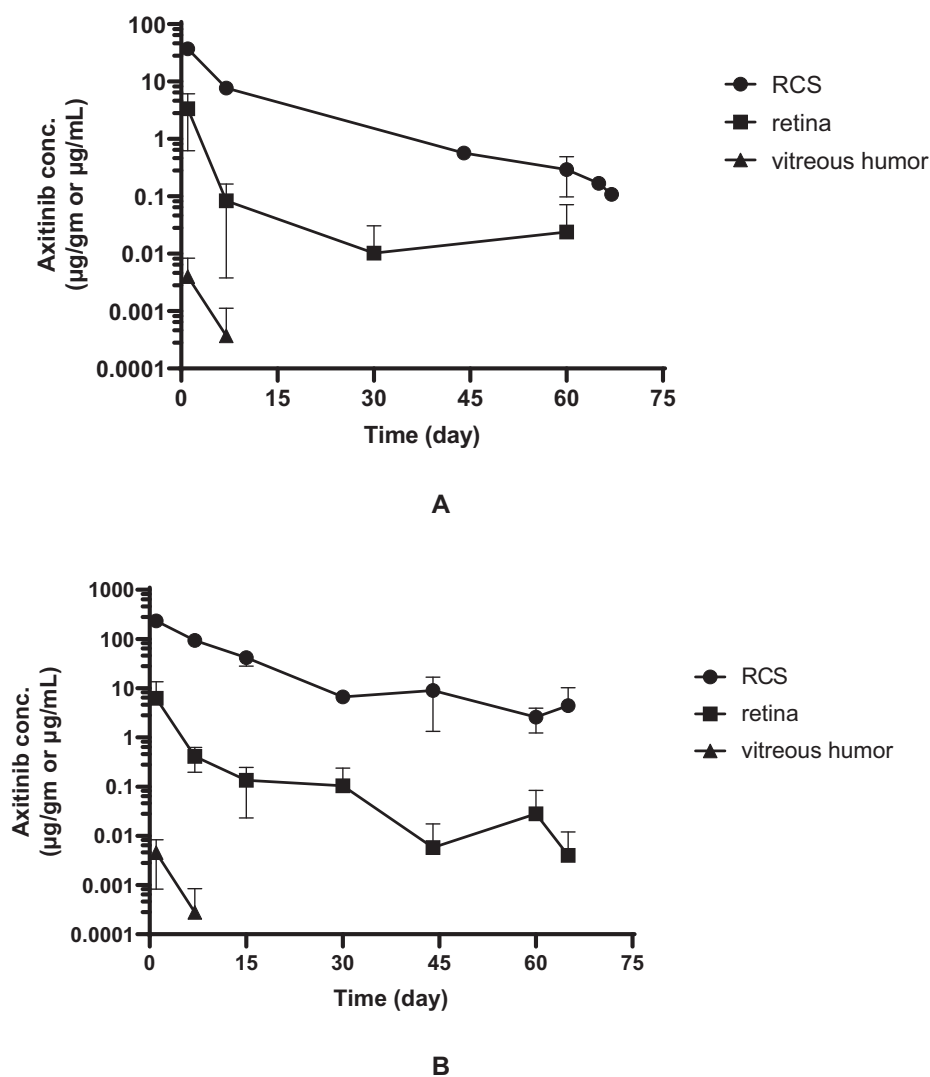


**Figure 4.** Concentration–time profiles of axitinib in the RCS, retina, and vitreous humor after a single bilateral administration of axitinib suspension at 0.03 mg/eye dose level (A) and at 0.1 mg/eye dose level (B) via SC injection in Dutch-Belted rabbits ( $n = 4$  eyes/2 rabbits/time point). Missing data points represent axitinib levels below level of detection at respective timepoints. Data are presented as mean  $\pm$  SD. Error bars smaller than the symbol size are not seen on the graph.

The durability of axitinib exposure in the chorioretina after a single bilateral SC injection of axitinib suspension was then assessed in a 13-week rabbit study (study 2). Sustained and high exposure of axitinib in chorioretinal tissues was observed during the entire study duration (91 days), while resulting in low exposure in the vitreous humor and below the LOQ in the aqueous humor and plasma. Although less therapeutically relevant in nAMD, even the retina concentrations of axitinib remained 5 log orders higher than the reported in vitro (VEGFR2 autophosphorylation inhibition assay) 50% inhibitory concentration value ( $0.5 \text{ nM} = 0.2 \text{ ng/mL}$ )<sup>54</sup> throughout the duration of this 91-day study.

Axitinib suspension spreads posteriorly and circumferentially toward the back of the eye after SC injection, and forms a sustained release drug depot adjacent to the choroid. From this SC depot, axitinib is slowly released over time yielding high levels of axitinib in the choroid and retina for months. The durability of the axitinib suspension depot (60% of injected dose on day 91), further supports the potential of suprachoroidally delivered axitinib suspension as a long-acting delivery system.

Axitinib is a potent inhibitor of VEGFR2 with picomolar inhibitory concentration<sup>12</sup>; therefore, ocular PK and the disposition of axitinib was further assessed at clinically relevant doses (0.03 and 0.10 mg/eye). In



this 10-week low-dose study, the dose depot (RCS) had 1 to 2 orders of magnitude higher axitinib levels than the retina, and the retina had 3 to 4 orders of magnitude higher axitinib levels than the vitreous humor. Although less therapeutically relevant in nAMD, even the sporadically detected axitinib levels in the retina were at least 20- 120-fold higher than the in vitro (VEGFR2 autophosphorylation assay) 50% inhibitory concentration value of axitinib (0.2 ng/mL),<sup>54</sup> throughout the duration of the study.

Similarly, in a separate 30-week rabbit toxicology study (see supplement), mean axitinib levels in the RCS and retina were 3–5 log orders higher than the in-vitro IC<sub>50</sub> value (0.2 ng/mL), on day 182 after a single 1.05 mg/eye SC injection.

This study has several limitations, including a small sample size, but it is consistent with prior studies assessing other therapeutic suspensions,<sup>55,56</sup> demonstrating prolonged highest levels in the RCS, with progressively lower levels in the retina, then vitreous, then aqueous, regardless of the dose assessed. The level of axitinib in the RCS and PEC include axitinib concentrations from axitinib suspension depot as well as soluble axitinib. The dose depot in the RCS, however, enables sustained release of axitinib into the therapeutically relevant choroidal and RPE; furthermore, the consistently high levels of axitinib in the RCS corroborate the sporadic levels observed in the retina at the lowest dose. Because rabbits do not have a macula, axitinib levels in the macula region were not specifically assessed in this study. However, optical coherence tomography-based imaging in rabbits undergoing SC injection of identical volumes has demonstrated acute opening of the SCS posteriorly to the optic nerve.<sup>57–59</sup> Nevertheless, given ocular anatomical differences between rabbits and humans, the clinical translatability of these rabbit PK data remains to be assessed.

## Conclusion

This research suggests that microneedle-based SC administration enables direct, high, and sustained delivery of axitinib to the therapeutically relevant choroid and RPE which may confer benefits in terms of durability and efficacy in nAMD, compared with topical or systemic administration. Moreover, SC administration enabled compartmentalized delivery of axitinib depot into the SCS that resulted in minimal to no exposure in the aqueous humor and systemic circulation, and may limit the possibility of off-target effects or axitinib suspension particles in the vitreous humor (snow-globe effect). Overall, these ocular PK

studies support the potential of SC axitinib suspension as a long-acting therapy for the treatment of patients with nAMD. Furthermore, the relatively high levels in the retina also support its potential as a treatment for retinal vascular disease such as diabetic retinopathy, retina vein occlusions and associated macular edema. If successful, this may address current treatment burden and suboptimal response to standard of care anti-VEGF-A therapies. Further studies are warranted.

## Acknowledgments

Disclosure: **V.S. Kansara**, Clearside Biomedical Inc. (E); **L.W. Muya**, Clearside Biomedical Inc. (E); **T.A. Ciulla**, Clearside Biomedical Inc. (E)

## References

1. Friedman DS, O'Colmain BJ, Muñoz B, et al. Prevalence of age-related macular degeneration in the United States. *Arch Ophthalmol*. 2004;122(4):564–572.
2. Congdon N, O'Colmain B, Klaver CCW, et al. Causes and prevalence of visual impairment among adults in the United States. *Arch*. 2004;122(4):477–485.
3. Wong WL, Su X, Li X, et al. Global prevalence of age-related macular degeneration and disease burden projection for 2020 and 2040: a systematic review and meta-analysis. *Lancet Glob Heal*. 2014;2(2):e106–e116.
4. Leung DW, Cachianes G, Kuang WJ, Goeddel DV, Ferrara N. Vascular endothelial growth factor is a secreted angiogenic mitogen. *Science*. 1989;246:1306–1309.
5. Ambati J, Ambati BK, Yoo SH, Ianchulev S, Adamis AP. Age-related macular degeneration: etiology, pathogenesis, and therapeutic strategies. *Surv Ophthalmol*. 2003;48(3):257–293.
6. Flaxel CJ, Adelman RA, Bailey ST, et al. Age-Related Macular Degeneration Preferred Practice Pattern. *Ophthalmology*. 2020;127(1):P1–P65.
7. Singer MA, Awh CC, Sadda S, et al. HORIZON: an open-label extension trial of ranibizumab for choroidal neovascularization secondary to age-related macular degeneration. *Ophthalmology*. 2012;119(6):1175–1183.
8. Maguire MG, Martin DF, Ying G-S, et al. Five-year outcomes with anti-vascular endothelial growth factor treatment of neovascular age-related

- macular degeneration: the comparison of age-related macular degeneration treatments trials. *Ophthalmology*. 2016;123(8):1751–1761.
9. Rofagha S, Bhisitkul RB, Boyer DS, Sadda SR, Zhang K. Seven-year outcomes in ranibizumab-treated patients in ANCHOR, MARINA, and HORIZON: a multicenter cohort study (SEVEN-UP). *Ophthalmology*. 2013;120(11):2292–2299.
  10. Ciulla TA, Hussain RM, Pollack JS, Williams DF. Visual acuity outcomes and anti-vascular endothelial growth factor therapy intensity in neovascular age-related macular degeneration patients: a real-world analysis of 49 485 eyes. *Ophthalmol Retin*. 2020;4(1):19–30.
  11. Rao P, Lum F, Wood K, et al. Real-world vision in age-related macular degeneration patients treated with single anti-VEGF drug type for 1 year in the IRIS Registry. *Ophthalmology*. 2018;125(4):522–528.
  12. Pfizer Labs I. Inlyta [package insert]. Published online 2012. Available at: [http://www.accessdata.fda.gov/drugsatfda\\_docs/label/2012/202324lbl.pdf](http://www.accessdata.fda.gov/drugsatfda_docs/label/2012/202324lbl.pdf). Accessed October 26, 2020.
  13. Kang S, Roh CR, Cho W-K, et al. Antiangiogenic effects of axitinib, an inhibitor of vascular endothelial growth factor receptor tyrosine kinase, on laser-induced choroidal neovascularization in mice. *Curr Eye Res*. 2013;38(1):119–127.
  14. Giddabasappa A, Lalwani K, Norberg R, et al. Axitinib inhibits retinal and choroidal neovascularization in in vitro and in vivo models. *Exp Eye Res*. 2016;145:373–379.
  15. Lledó Riquelme M, Campos-Mollo E, Fernández-Sánchez L. Topical axitinib is a potent inhibitor of corneal neovascularization. *Clin Experiment Ophthalmol*. 2018;46(9):1063–1074.
  16. Yuan X, Marcano DC, Shin CS, et al. Ocular drug delivery nanowafer with enhanced therapeutic efficacy. *ACS Nano*. 2015;9(2):1749–1758.
  17. Shi S, Peng F, Zheng Q, et al. Micelle-solubilized axitinib for ocular administration in anti-neovascularization. *Int J Pharm*. 2019;560:19–26.
  18. Nakano A, Nakahara T, Mori A, Ushikubo H, Sakamoto K, Ishii K. Short-term treatment with VEGF receptor inhibitors induces retinopathy of prematurity-like abnormal vascular growth in neonatal rats. *Exp Eye Res*. 2016;143:120–131.
  19. Kaiser PK, Ciulla T, Kansara V. Suprachoroidal CLS-AX (axitinib injectable suspension), as a potential long-acting therapy for neovascular Age-Related Macular Degeneration (nAMD). *Invest Ophthalmol Vis Sci*. 2020;61(7):3977.
  20. MacCumber M. Suprachoroidal administration of small molecule and nanoparticle suspensions: pre-clinical results correlate to clinical trial outcomes. *Conference presentation at the Virtual Annual Macula Society Meeting*; Feb 6-7, 2021.
  21. Lieu CH, Tran H, Jiang Z-Q, et al. The association of alternate VEGF ligands with resistance to anti-VEGF therapy in metastatic colorectal cancer. *PLoS One*. 2013;8(10):e77117.
  22. Cabral T, Lima LH, Luiz LG, et al. Bevacizumab injection in patients with neovascular age-related macular degeneration increases angiogenic biomarkers. *Ophthalmol Retin*. 2018;2(1):31–37.
  23. Opthea Limited. OPT-302 Phase 2b in wet AMD. Available at: [https://www.opthea.com/wp-content/uploads/2019/09/20190905-EuRetina-ASX-Slides\\_Final2.pdf](https://www.opthea.com/wp-content/uploads/2019/09/20190905-EuRetina-ASX-Slides_Final2.pdf). Accessed October 26, 2020.
  24. Einmahl S, Savoldelli M, D’Hermies F, Tabatabay C, Gurny R, Behar-Cohen F. Evaluation of a novel biomaterial in the suprachoroidal space of the rabbit eye. *Invest Ophthalmol Vis Sci*. 2002;43(5):1533–1539.
  25. Gilger BC, Salmon JH, Wilkie DA, et al. A novel bioerodible deep scleral lamellar cyclosporine implant for uveitis. *Invest Ophthalmol Vis Sci*. 2006;47(6):2596–2605.
  26. Olsen TW, Feng X, Wabner K, et al. Cannulation of the suprachoroidal space: a novel drug delivery methodology to the posterior segment. *Am J Ophthalmol*. 2006;142(5):777–787.
  27. Kim SH, Galbañ CJ, Lutz RJ, et al. Assessment of subconjunctival and intrascleral drug delivery to the posterior segment using dynamic contrast-enhanced magnetic resonance imaging. *Invest Ophthalmol Vis Sci*. 2007;48(2):808–814.
  28. Patel SR, Berezovsky DE, McCarey BE, Zarnitsyn V, Edelhofer HF, Prausnitz MR. Targeted administration into the suprachoroidal space using a microneedle for drug delivery to the posterior segment of the eye. *Invest Ophthalmol Vis Sci*. 2012;53(8):4433–4441.
  29. Yeh S, Khurana RN, Shah M, et al. Efficacy and safety of suprachoroidal CLS-TA for macular edema secondary to noninfectious uveitis: phase 3 randomized trial. *Ophthalmology*. 2020;127(7):948–955.
  30. Wan C, Kapik B, Wykoff CC, et al. Clinical characterization of suprachoroidal injection procedure utilizing a microinjector across three retinal disorders. *Transl Vis Sci Technol*. 2020;9(11):27, doi:10.1167/tvst.9.11.27.
  31. Kwak HW, D’Amico DJ. Evaluation of the retinal toxicity and pharmacokinetics of dexamethasone after intravitreal injection. *Arch Ophthalmol*. 1992;110(2):259–266.

32. Kane FE, Green KE. Ocular pharmacokinetics of fluocinolone acetonide following iluvien implantation in the vitreous humor of rabbits. *J Ocul Pharmacol Ther.* 2015;31(1):11–16.
33. Kim HM, Park YJ, Lee S, et al. Intraocular pharmacokinetics of 10-fold intravitreal ranibizumab injection dose in rabbits. *Transl Vis Sci Technol.* 2020;9(4):7.
34. Kernt M, Thiele S, Liegl RG, et al. Axitinib modulates hypoxia-induced blood-retina barrier permeability and expression of growth factors. *Growth Factors.* 2012;30(1):49–61.
35. Thiele S, Liegl RG, König S, et al. [Multikinase inhibitors as a new approach in neovascular age-related macular degeneration (AMD) treatment: in vitro safety evaluations of axitinib, pazopanib and sorafenib for intraocular use]. *Klin Monbl Augenheilkd.* 2013;230(3):247–254.
36. Holz FG, Tadayoni R, Beatty S, et al. Multi-country real-life experience of anti-vascular endothelial growth factor therapy for wet age-related macular degeneration. *Br J Ophthalmol.* 2015;99(2):220–226.
37. Ciulla TA, Huang F, Westby K, Williams DF, Zaveri S, Patel SC. Real-world outcomes of anti-vascular endothelial growth factor therapy in neovascular age-related macular degeneration in the United States. *Ophthalmol Retin.* 2018;2(7):645–653.
38. Holekamp NM, Liu Y, Yeh W-S, et al. Clinical utilization of anti-VEGF agents and disease monitoring in neovascular age-related macular degeneration. *Am J Ophthalmol.* 2014;157(4):825–833.e1.
39. Brown DM, Michels M, Kaiser PK, Heier JS, Sy JP, Ianchulev T. Ranibizumab versus verteporfin photodynamic therapy for neovascular age-related macular degeneration: two-year results of the ANCHOR study. *Ophthalmology.* 2009;116(1):57–65.e5.
40. Busbee BG, Ho AC, Brown DM, et al. Twelve-month efficacy and safety of 0.5 mg or 2.0 mg ranibizumab in patients with subfoveal neovascular age-related macular degeneration. *Ophthalmology.* 2013;120(5):1046–1056.
41. Schmidt-Erfurth U, Kaiser PK, Korobelnik J-F, et al. Intravitreal aflibercept injection for neovascular age-related macular degeneration: ninety-six-week results of the VIEW studies. *Ophthalmology.* 2014;121(1):193–201.
42. Heier JS, Brown DM, Chong V, et al. Intravitreal aflibercept (VEGF trap-eye) in wet age-related macular degeneration. *Ophthalmology.* 2012;119(12):2537–2548.
43. Rosenfeld PJ, Brown DM, Heier JS, et al. Ranibizumab for neovascular age-related macular degeneration. *N Engl J Med.* 2006;355(14):1419–1431.
44. ClinicalTrials.gov. Open-label, pilot study of TG100801 in patients with choroidal neovascularization due to AMD. ClinicalTrials.gov. Published 2008. Available at: <https://clinicaltrials.gov/ct2/show/NCT00509548>. Accessed October 29, 2020.
45. Csaky KG, Dugel PU, Pierce AJ, et al. Clinical evaluation of pazopanib eye drops versus ranibizumab intravitreal injections in subjects with neovascular age-related macular degeneration. *Ophthalmology.* 2015;122(3):579–588.
46. Jousseaume AM, Wolf S, Kaiser PK, et al. The Developing Regorafenib Eye drops for neovascular Age-related Macular degeneration (DREAM) study: an open-label phase II trial. *Br J Clin Pharmacol.* 2019;85(2):347–355.
47. Adams CM, Anderson K, Artman G, 3rd, et al. The discovery of N-(1-Methyl-5-(trifluoromethyl)-1H-pyrazol-3-yl)-5-((6-(methylamino)methyl)pyrimidin-4-yl)oxy)-1H-indole-1-carboxamide (Acrizantib), a VEGFR-2 inhibitor specifically designed for topical ocular delivery, as a therapy for neovascular age. *J Med Chem.* 2018;61(4):1622–1635.
48. Dugel PU. Reframing the retina pipeline. *Retin Today.* 2019;(December):21–24. Available at: <https://retinatoday.com/articles/2019-nov-dec/reframing-the-retina-pipeline>. Accessed October 26, 2020.
49. Aziz Aamir, Khan Majid, Shafi Noah, Khanani A. Sustained-release sunitinib malate for neovascular age-related macular degeneration. Available at: <https://www.retinalphysician.com/issues/2020/march-2020/sustained-release-sunitinib-malate-for-neovascular>. Accessed October 26, 2020.
50. GlobeNewswire. Graybug vision concludes patient enrollment in its phase 2b clinical trial of GB-102 in wet age-related macular degeneration and accelerates trial read-out by approximately six months. Available at: <https://www.globenewswire.com/news-release/2020/03/18/2002492/0/en/Graybug-Vision-Concludes-Patient-Enrollment-in-its-Phase-2b-Clinical-Trial-of-GB-102-in-Wet-Age-Related-Macular-Degeneration-and-Accelerates-Trial-Read-out-by-Approximately-Six-Mon.html>. Accessed October 27, 2020.
51. Chaney P. PAN-90806: once-daily topical anti-VEGF eye drop for wet AMD and other neovascular eye disease. *Ophthalmology Innov Summit, Oct 10, 2019, San Fr CA.* Published online 2019.

- Available at: <https://www.panopticapharma.com/wp-content/uploads/2019/10/PAN-90806-Data-at-OIS@AAO.pdf>. Accessed October 27, 2020.
52. Cousins S. Topical treatment for neovascular AMD within sight. *Modern Retina*. Published 2016. Available at: <https://www.modernretina.com/view/topical-treatment-neovascular-amd-within-sight>. Accessed October 29, 2020.
  53. Avery R. Safety and efficacy of OTX-TKI, a novel tyrosine kinase inhibitor hydrogel intravitreal implant. Phase 1 trial interim review. Published online 2019, <http://docplayer.net/187439409-Safety-and-efficacy-of-otx-tki-a-novel-tyrosine-kinase-inhibitor-hydrogel-intravitreal-implant.html>. Accessed October 27, 2020.
  54. Hu-Lowe DD, Zou HY, Grazzini ML, et al. Non-clinical antiangiogenesis and antitumor activities of axitinib (AG-013736), an oral, potent, and selective inhibitor of vascular endothelial growth factor receptor tyrosine kinases 1, 2, 3. *Clin Cancer*. 2008;14(22):7272–7283.
  55. Burke B, Patel SR, Taraborelli D, Struble CB, Noronha G. Targeted delivery of triamcinolone acetonide and CLS011A to the posterior ocular tissues via suprachoroidal administration. *Invest Ophthalmol Vis Sci*. 2017;58(8):4112.
  56. Edelhauser H, Patel S, Meschter C, Dean R, Powell K, Verhoeven R. Suprachoroidal microinjection delivers triamcinolone acetonide to therapeutically-relevant posterior ocular structures and limits exposure in the anterior segment. *Invest Ophthalmol Vis Sci*. 2013;54(15):5063.
  57. Jung JH, Desit P, Prausnitz MR. Targeted drug delivery in the suprachoroidal space by swollen hydrogel pushing. *Invest Ophthalmol Vis Sci*. 2018;59(5):2069–2079.
  58. Patel SR, Lin ASP, Edelhauser HF, Prausnitz MR. Suprachoroidal drug delivery to the back of the eye using hollow microneedles. *Pharm Res*. 2011;28(1):166–176.
  59. Kansara V. Suprachoroidally delivered DNA nanoparticles transfect retina and RPE/choroid in rabbits. *Transl Vis Sci Technol*. 2020;9:21.